Nano Research
2023, 16(12): 13029–13041

ISSN 1998-0124 CN 11-5974/O4
https://doi.org/10.1007/s12274-023-5766-z

Review Article

Endogenous formaldehyde responsive fluorescent probe for bioimaging

Ning-Bo Yi[1,2], Xing-Jie Hu[2], Fei Wang[3], Si-Yi Chen[1], Xiao-Xue Xu[1], Xin Li[1], Hao Wang[2], Taolei Sun[1], Zeng-Ying Qiao[2] (✉), and Dong-Bing Cheng[1] (✉)

[1] *Hubei Key Laboratory of Nanomedicine for Neurodegenerative Diseases, School of Chemistry, Chemical Engineering & Life Science, Wuhan University of Technology, Wuhan 430070, China*
[2] *CAS Center for Excellence in Nanoscience Laboratory for Biological Effects of Nanomaterials and Nanosafety, National Center for Nanoscience and Technology (NCNST), Beijing 100190, China*
[3] *Department of Biology and the School of Natural Sciences, Went Worth College, University of York, Heslington, York, YO10 5DD, UK*

Received: 14 March 2023 / **Revised:** 18 April 2023 / **Accepted:** 20 April 2023

ABSTRACT

Formaldehyde (FA), as the simplest endogenous carbonyl molecule, participates in many biosynthesis and metabolism in living organisms, such as nucleotides and adenosine triphosphate (ATP). FA concentrations are sub-millimolar in the normal healthy body, but can rise significantly in a number of disease pathologies. As a result, detecting endogenous FA is critical for illness diagnosis and rehabilitation therapy monitoring. Recent studies have focused on the FA-responsive turn-on fluorescence probe, which has huge promise in the detection and visualization of FA in living cells and organisms, as well as exceptional use in disease diagnosis and therapeutic monitoring. This review summarizes the fluorescence luminescence mechanism and design concepts of FA fluorescent probes, as well as their recent applications in bioimaging and illness diagnostics. Additionally, this article indicates the present dilemma of FA-responsive fluorescent probe, including selectivity, specificity, and detection mode, which may provide references for the development of FA-responsive fluorescent probes.

KEYWORDS

endogenous formaldehyde, fluorescent probe, tumor cell, bioimaging

1 Introduction

The World Health Organization has included formaldehyde (FA), the most basic reactive carbonyl and aldehyde found in nature [1], on its list of Group I carcinogens due to its toxicity and cancer-causing potential. Excessive exposure to FA deteriorates memory and increases the risk of acquiring dozens of diseases, including cancer, diabetes, and asthma [2]. FA has harmful effects on the cardiovascular and reproductive systems and can cause disruption of the human endocrine system [3]. According to the research by Burgos-Barragan's team, the oxidative breakdown of tetrahydrofolic acid and folic acid in the human body results in the production of FA, and the cleavage of serine by serine hydroxymethyltransferase leads to the production of endogenous FA [4, 5]. FA is labeled with C13 isotope, and experimental results show that FA is involved in nucleotide synthesis and promotes adenosine triphosphate (ATP) synthesis [6]. In addition, the overexpression of endogenous FA may lead to neurodegenerative diseases such as Alzheimer's disease [7]; FA can decrease superoxide dismutase activity, thereby damaging cardiomyocytes; excess FA can cause endothelial cell damage and apoptosis; and excess endogenous FA can crosslink with DNA strands, leading to decreased stability of DNA strands. Thus, excess endogenous FA will generate an increased incidence of diseases such as dwarfism, Fanconi anemia, and cancer [8–10].

Under normal conditions, endogenous FA generation and consumption *in vivo* are usually dynamically balanced at the sub-millimolar level. However, in the event of disease occurrence or other external factors, the level of endogenous FA in the body may exceed normal levels. Lots of studies have shown a strong association between excess FA and many diseases, wherein the dynamic equilibrium of endogenous FA is disrupted, and its level of FA concentration increases to 2–8 times approximately [11, 12]. Typically, the level of endogenous FA is elevated in cancer tissue. Therefore, the exploration of an efficient detection method for FA is strongly necessary for disease diagnosis and rehabilitation therapy monitoring.

Currently, FA detection methods based on mass spectrometry, chromatography, colorimetry, electrochemistry, and fluorescence methods have been continuously developed [13–26]. Among them, FA fluorescence detection method has attracted more and more attention because of its non-invasiveness, high sensitivity, and outstanding interference suppression ability. For example, high-performance liquid chromatography (HPLC) and colorimetry detection method have the advantage of sensitivity and wider inspection range, but they cannot be used to detect FA in organisms. High precision and sensitivity are benefits of mass spectrometry and gas chromatography, while the disadvantage is the cumbersome operation and sample pretreatment. Electrochemical methods have high specificity response and can

Address correspondence to Zeng-Ying Qiao, qiaozy@nanoctr.cn; Dong-Bing Cheng, chengdb@whut.edu.cn

be output as digital signal, but they are not applicable in turbid samples and have low quantum yield. These strategies were all used to quickly screen for FA in biological materials. However, none of them can be used to directly diagnose and identify specific diseases, nor are they appropriate for the genuine analysis of endogenous FA production. The fluorescence methods can overcome the above limitations, which show simplicity and quickness, as well as high sensitivity to changes in endogenous FA in timely manner without causing harm to the organism. In order to detect FA, fluorescent probe design and construction are therefore crucial.

Many *in situ* chemical reactions of FA can realize fluorescence turn-on, suggesting the potential for FA-responsive bioimaging. However, the clinical application of endogenous FA fluorescent probes should consider: (i) high selectivity, high specificity with FA, and minimal to no reaction to physiologically significant aldehyde-containing species including acetaldehyde, glucose, and methylglyoxal; (ii) good tissue permeability, which can enter into tumor cells stably, and respond with endogenous FA; and (iii) low systemic toxicity and no damage to cells. Up to now, most reported chemical reactions of FA with clinical potential can be divided into three categories, including (1) 2-aza-cope rearrangement reaction, which converts the high allyl amine group into an aldehyde group; (2) condensation of $-NH_2$ and FA to form a formyl imide; and (3) reaction of $-NHNH_2$ and FA to form hydrazone (Fig. 1). As a result, under this review, we highlight the present research development of FA fluorescent probes that can be utilized for bioimaging, as well as address their biological applications in illness detection. The design philosophy and construction techniques of FA probes in terms of responsive turn-on attributes are also focused on. Besides, current endogenous FA fluorescence turn-on mechanisms are illustrated and thoroughly investigated. Ultimately, we hope to provide researchers with a deep understanding of the construction of FA fluorescence turn-on probes and anticipate achieving a novel FA fluorescent probe with higher imaging quality to reveal the intrinsic connection between endogenous FA and diseases.

2 Luminescence mechanism

Researchers have long utilized photo-induced electron transfer (PET), intramolecular charge transfer (ICT), excited state intramolecular proton transfer (ESIPT), and fluorescence resonance energy transfer (FRET) to design fluorescent probes.

The probe structure based on PET mechanism includes fluorescence group and recognition group. The recognition group contains electron donor group, which is not conjugated with fluorescence group through unsaturated bond, but is connected with fluorescence group by σ-bond [27]. PET mechanisms are classified as reductive-PET or oxidative-PET based on the distribution of molecular orbitals prior to the binding of fluorescent probe molecules. The reductive-PET mechanism states that the fluorescent group is excited when the highest occupied molecular orbital (HOMO) energy level of the probe's intramolecular recognition group exceeds the HOMO amount of energy of the fluorescent group. When the electron transitions to the lowest unoccupied molecular orbital (LUMO), the electron donor group in the recognition group transitions from the fluorescent group's HOMO to the fluorescent group's HOMO, preventing the electron in the fluorescent group's LUMO from transitioning to the ground state and causing fluorescence quenching. The oxidative-PET mechanism is similar. As the electrons of the excited fluorescent group may not go to the ground state but to the LUMO of the recognizing group, fluorescence is quenched when the LUMO energy level of the recognizing group is lower compared with the fluorescent group. When the identification group reacts with the material to be evaluated, its energy level changes, so that the identification group's LUMO energy level is higher than that of the fluorescent group. The recognition group's HOMO energy level is lower than that of the fluorescence group, and the fluorescence transition is normal, which prevents the formation of PET and subsequently lights up the fluorescence [28–31].

ICT is a probe molecule based on intramolecular charge transfer, and its structure contains three parts: an electron-absorbing group (A), an electron-donating group (D) with a conjugated structure, and a fluorophore. The three units form a large D–π–A conjugated system, and the electron-donating group can transfer electrons to the electron-absorbing group due to the conjugation effect [32]. The electron-donor state of the probe molecule and the HOMO of the electron-absorbing group are both filled with electrons in the initial state, however its LUMO is empty. At this time, the probe molecule's electron donor group will transfer electrons from the HOMO of the electron donor group to the LUMO of the electron absorption group via intramolecular charge transfer. Because the molecule is unstable in the excited state, it will produce fluorescence in the form of radiation when it recovers to the initial state [33]. And because the aromatic plane is small, it can effectively reduce the excitation interference and thus improve the imaging quality [34].

The probe molecules of the ESIPT mechanism have enolic and

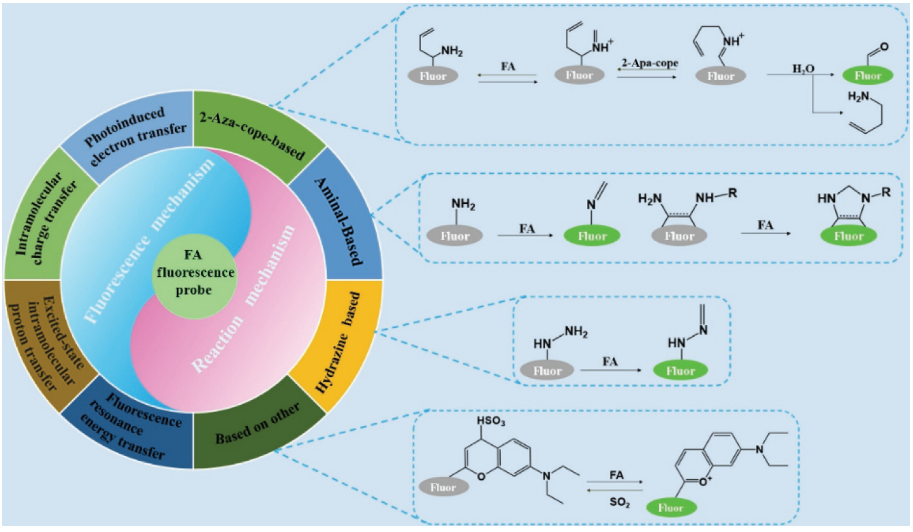

Figure 1 The luminescence mechanism and the FA-responsive turn-on fluorescent probe.

ketonic reciprocal isomerism. ESIPT fluorescence refers to the luminescence mechanism of the interaction between intramolecular hydrogen-bonded donor and acceptor [35, 36]. When the molecule exists in the enol form, the heteroatoms inside the molecule form stable hydrogen bonds, but when the molecule receives an exciting leap to the enol excited state, the proton inside the molecule is transferred to another heteroatom, which undergoes rearrangement, leading to the enol–keto interconversion isomerization and the molecule transitions to an agitated ketosis isomer state. Following the enol–keto isomerization, the electron leaps toward the ketoisomeric initial state and returns to enol base state. In comparison with directly emitted fluorescence photons, the ESIPT method emits lower fluorescence energy and seems to have a significant Stokes shift, great selectivity, as well as the capacity to avoid interference from other fluorescence signals [37, 38].

FRET is a photophysical phenomenon, which refers to the physical process that enables the non-radiative transferring energy with an energized molecular chromophore to another chromophore through long-range intermolecular dipole–dipole coupling [39]. FRET occurs between the donor and recipient at a distance of 10 to 100 Å [40, 41]. The efficiency of energy transmission increases with decreasing distance and increasing spectral overlap between the donor and the receiver [42, 43].

3 FA-responsive turn-on fluorescent probe

3.1 Fluorescence turn-on depending upon 2-aza-cope rearrangement

2-Aza-cope rearrangement reaction is a process in which an aza-1,5-diene is isomerized by [3,3]-σ rearrangement [44]; the high allylamine moiety of the FA in the probe is condensed with FA and reacted by 2-aza-cope rearrangement with hydrolysis to provide an aldehyde or ketone with strong fluorescence [45]. Furthermore, when compared with other reactive carbonyl compounds, the 2-aza-cope rearrangement mechanism exhibits great selectivity and specificity with FA, allowing for the development of FA fluorescent probes (Fig. 2).

Roth's and Brewer's teams are independent of each other, and the 2-aza-cope rearrangement reaction was applied simultaneously in the construction of a fluorescent probe of FA for the initial time [46, 47]. Brewer's group created the FAP-1 FA fluorescent probe, which uses aminomethylsilanolamine dye like a fluorescence and homoallylamine as an FA reaction site (Fig. 3(d)). The fluorescence intensity increased 8 times after 1 h of FA contact with the probe, and 45 times with incubation period extension. The fluorescence intensity of FA is dose-dependent with that of FAP-1 within the range of physiological dissolution of living cells, and endogenous FA can be identified in illness models (Fig. 3).

Meanwhile, Roth's team designed a fluorescent probe FP1 with a silicone Rhodol dye as a fluorescent scaffold, 4-nitrobenzyl as a bursting agent, and a high allylamine reacting with FA [46], where the d-PET effect of 4-nitrobenzyl makes the probe FP1 non-fluorescent before FA treatment, reducing the background fluorophores of FP1. After 2-aza-cope rearrangement and hydrolysis reaction, the PET effect is ended when FP1 is attached to FA, and the probe exhibits intense fluorescence (Fig. 4). The fluorescence intensity of the sensor grew to 7 times after 3 h when the FA solubility was 0.25 mM, and the expression level of FP1 increased as the FA solubility increased. When FA solubility is 5 mM, the fluorescence intensity can reach 33.5 times after 3 h. And the probe FP1 showed low or no response with bio-relevant aldehyde-containing species such as acetaldehyde, glucose,

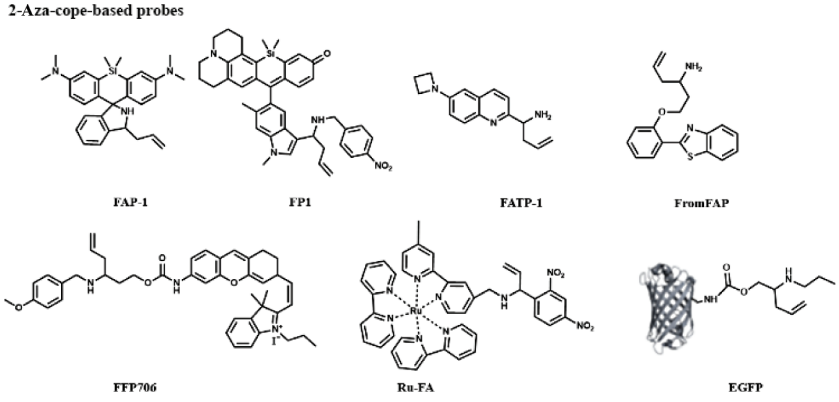

Figure 2 Chemical structure of FA probe based on 2-aza-cope probes.

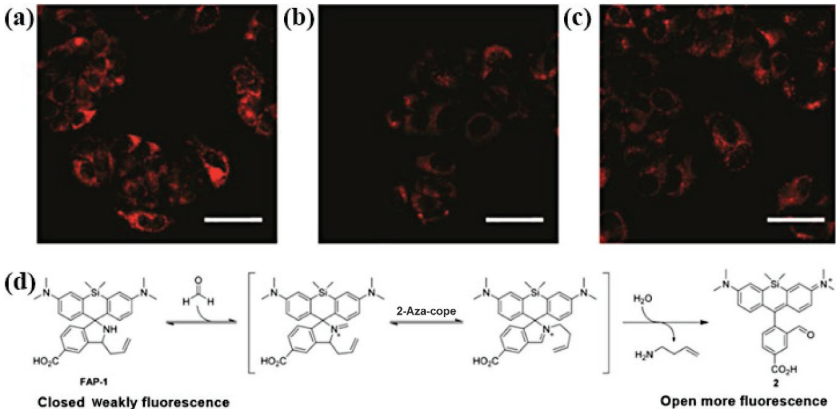

Figure 3 (a) FAP-1-treated MCF7 cells as seen by confocal microscopy. (b) 20 μM tranylcypromine (TCP). Reproduced with permission from Ref. [48], © Elsevier Ltd. 2016. (c) 1 μM GSK-lysine-specific demethylase 1 (LSD1).Reproduced with permission from Refs. [49, 50] © Liu, J. et al. 2013 and Taylor & Francis 2016. Scale bar: 50 μm. Blockers for LSD1 include TCP and GSK-LSD1. Inhibiting the production of LSD1 can reduce the production of endogenous FA. (d) Chemical structure diagram of FAP-1 fluorescent lighting. Reproduced with permission from Ref. [47], © American Chemical Society 2015.

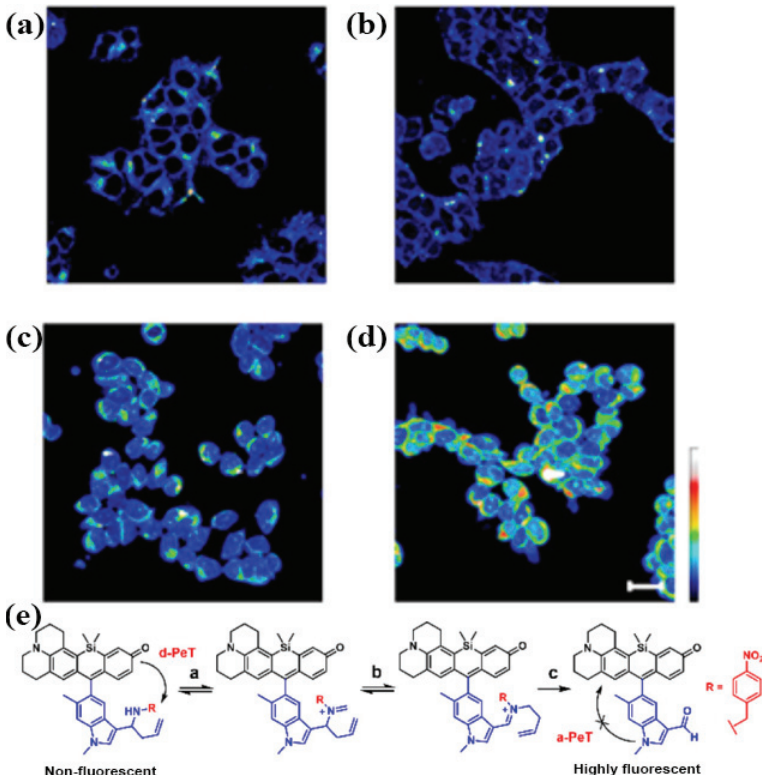

Figure 4 Pictures of HEK293TN cells taken with a confocal microscope. HEK293TN cells were pretreated with 2 μM FP1, and then treated with FA with different solubility. (a) 0 mM, (b) 1 mM, (c) 2.5 mM, and (d) 5 mM. Scale bar: 20 μm. (e) Chemical structure diagram of FP1 fluorescent lighting. Reproduced with permission from Ref. [46], © American Chemical Society 2015.

methylglyoxal, and pyridoxal, proving that FP1 has excellent selectivity. The probe FP1 did not react with intracellular thiol-reducing chemicals like glutathione, glutathione (GSH), and sulfur oxides, nor with hydrogen peroxide oxidizing molecules, showing that FP1 is chemically stable under physiological conditions. The fluorescence did not decrease after 100 scans at 25% laser power, demonstrating the excellent photostability of the probe FP1. FP1 exhibited good dose-dependent properties by treating cells with different FA solubilities.

Chen's lab originally created a two-photon FA fluorescent probe (FATP-1) and utilized it to detect endogenous FA in cells, nematodes, and mice brain tissue with robust fluorescence imaging and low toxic effects [51]. The quinoline structure in the probe gives it strong penetration into deep cellular tissues and two-photon excitation properties. The 2-aza-cope reaction, which uses allylamine as a recognition group for FA, affords the probe great selectivity with FA as well as strong cellular permeability. The aza-heterocycle was converted into an electron-donating group by nitrogen-containing rings of various sizes, which improved the fluorophore's brightness and photostability while preserved its spectral characteristics and cell permeability. After the probe FATP-1 was reactivated with FA, the most significant fluorescence intensity increased by about 46 times, which indicated that nitrogen heterocyclic substitution could effectively reduce the internal charge transfer of the probe and improve the fluorescence brightness. The blood–brain boundary was not an obstacle for FATP-1 as it tracked the dynamic FA changes within the brains of mice with epilepsy (mice with epilepsy induced by intraperitoneal injection of kainite) [52] in real-time (Fig. 5). The results of the experiment demonstrated that epilepsy causes abnormal elevation of endogenous FA and harm to the brain's neurons and that inhibiting abnormally elevated endogenous FA can lessen this injury.

N-p-Methoxybenzyl high allylamine was found to have a more potent azetidine reactivity toward FA by Du et al. [53] when they designed and compared the fluorescence responses of a number of N-substituted high allylamine coumarin probes to FA. The intensity of the fluorescence was significantly larger; density functional theory (DFT) calculations of the reaction of N-substituted higher allylamines with FA revealed that enhanced fluorescence of the coumarin probe towards FA could be determined by the condensation step compared to the 2-aza-cope rearrangement. The cytotoxicity of the FFP706 probe can be ignored in the range of working solubility, confocal microscopy of the FFP706 probe can detect changes in intracellular FA levels in living cells, and because of the overexpression of endogenous FA in brain tissue, mouse brain sections were incubated with an FFP706 probe. FFP706 has the capability to image intrinsic FA in live tumor tissues using confocal microscopy. By injecting the FFP706 probe into regions of tumors in live mice, fluorescence imaging was about 5 times that of normal cells. The FFP706 probe has a low detection limit, good sensitivity, good water hydrophilicity, and a near-infrared (NIR) fluorescent wavelength of 706 nm, allowing it to be used in a variety of biological applications in live cells, tissues, and also mice. Zhang et al. [54] developed an active gene editing-based fluorescent probe for detecting endogenous FA. The probe blends FA's 2-aza-cope sensitivity with protein engineering enhanced green fluorescent protein (EGFP) and firefly luciferase neutralization regulation in an organic manner. The probe is applied to analyze endogenous FA through living mammalian cells, which offers a novel approach to the design of an FA fluorescent probe.

Liu et al. [55] developed a dual-key FA fluorescence probe Ru-FA, which shows fluorescence only in the combined action of an acidic microenvironment and FA. It not only prevents false-positive probe fluorescence but also reduces interference fluorescence of heterosignal, and makes Ru-FA lysosomal-targeted (Fig. 6(a)). The probe's Ru(II) complex functions like a chromophore, and 2,4-dinitrobenzene functions like a bursting group, which inhibits the expression of the fluorophore through

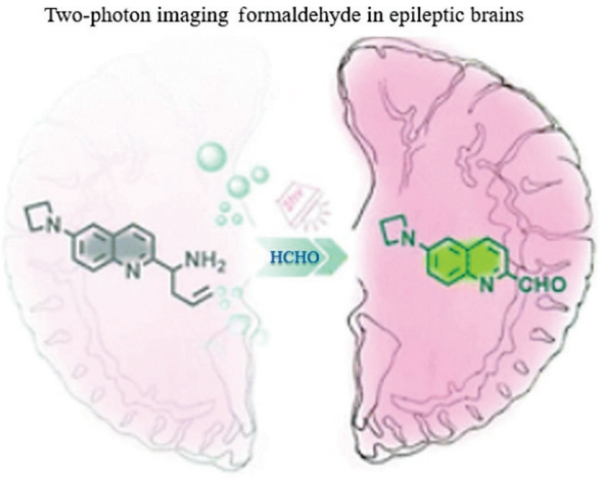

Figure 5 Design and imaging principles of the two-photon probe FATP-1. Reproduced permission from Ref. [51], © American Chemical Society 2020.

its electron-absorbing and photoelectron-transfer effects, making the probe show weak fluorescence before responding with FA. The probe Ru-FA was added together with FA and exhibited strong fluorescence in the range of pH 3–6. It was demonstrated that Ru-FA can only react with FA and exhibit strong fluorescence in acidic environment. A pH of 4–6 inside the lysosomes of cells is favorable for the probe's fluorescence expression [56]. The fluorescence intensity of the probe Ru-FA showed a nice positive linear correlation with the solubility of FA, Ru-FA can detect endogenous FA in HeLa cells with exceptional specificity, and the detection concentration is as low as 19.8 nm (Fig. 6(b)). Liu et al. used sensors to identify the solubility of endogenous FA in mouse blood and major organs, with the brain having three times the FA content of the liver, indicating that probe Ru-FA is useful for the identification and quantification of FA. After pretreatment of tumor areas of mice with $NaHSO_3$ solution (a scavenger of FA) and injection of the Ru-FA probe, the areas treated with $NaHSO_3$ solution were weakly fluorescent and the areas not treated were strongly fluorescent, indicating that the Ru-FA probe is capable of detecting endogenous FA and has the potential to be used as a fluorescent probe for imaging in living organisms (Fig. 6(c)). Chen's group [57] developed their probe FormAFP, depending on the ESIPT effect, using 2-(2'-hydroxy-phenyl) benzothiazole (HBT) as a fluorophore and high allylamine as little more than a responsive site for FA. FormAFP responds to FA and is accompanied by β-elimination of allyl aldehyde after 2-aza-cope rearrangement to obtain HBT, which fluoresces based on the ESIPT fluorescence mechanism due to its intramolecular hydrogen bonding. The probe FormAFP has an ultra-fast response characteristic and can illuminate fluorescence within 10 min. The probe's reaction with FA produces hydrophobic molecules of HBT, which self-assemble in an aqueous solution to form nanoparticles with an average diameter of 398 nm, thereby decreasing the amount of material of the products in the solution phase, accelerating the reaction, increasing the conversion rate of the reaction, and achieving a rapid response. The solution's fluorescence intensity rose by as much as 240-fold after being treated with 1 mM FA, and its detection limit was 66 nM, enabling the rapid detection of intracellular FA solubility within 15 min and the precise detection of changes in endogenous FA due to oxidative stress stimulation in cells.

3.2 Fluorescence turn-on based on formylimine generation

The probe has an amino group and a fluorescent group, and the probe quenches its fluorescence under the action of photoinduced electron transfer or internal charge transfer. When the probe's amine group interacts with FA to establish a formylimine group, the fluorescence is restored as the inhibited electron interaction is lifted. Yoon's group [58] first proposed a fluorescent probe for FA detection in 2012 (Fig. 7) and opened up the possibility of biological applications for later generations. The probe uses BODIPY as a fluorophore and explains the optical properties of the probe AnB by molecular orbital energy level theory. Yang's group [59] modified the near-infrared fluorophore IR780 [60] to construct the amine-based near-infrared FA fluorescent probe probe-NH_2, whose fluorophore has a fluorescence emission of 708 nm and is capable of imaging THF-induced endogenous FA production in mice.

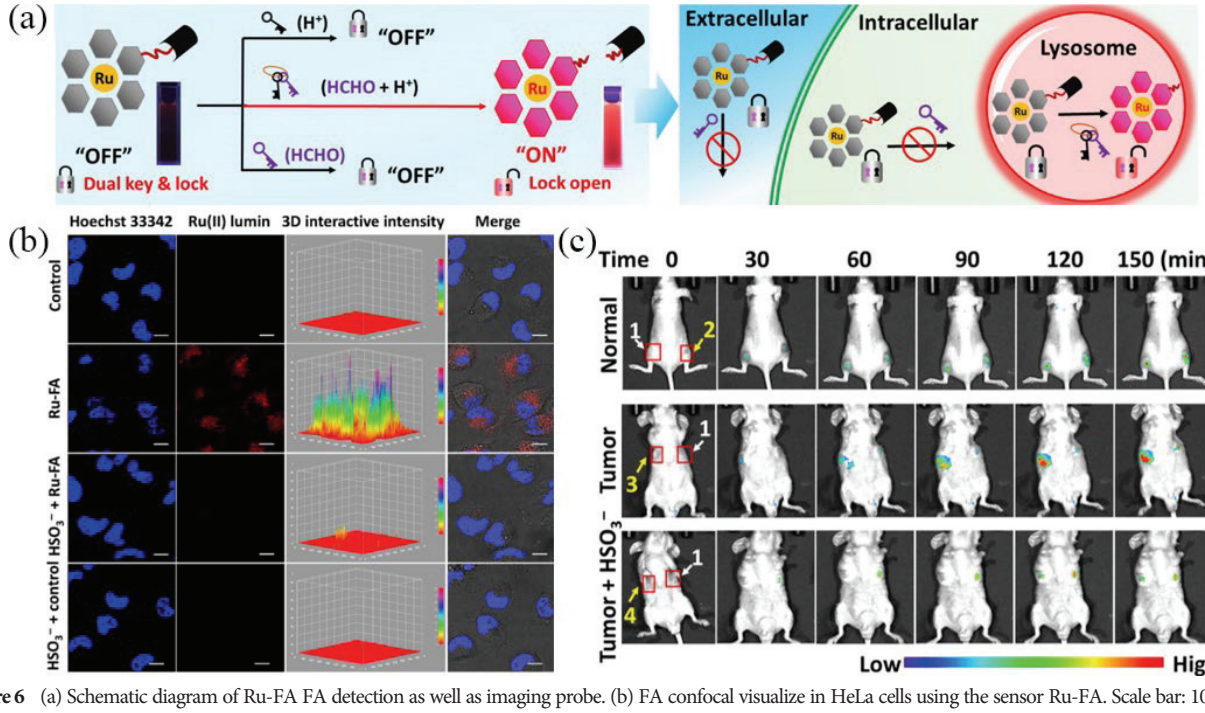

Figure 6 (a) Schematic diagram of Ru-FA FA detection as well as imaging probe. (b) FA confocal visualize in HeLa cells using the sensor Ru-FA. Scale bar: 10 μm. (c) Analyzing endogenous FA through imaging in healthy and tumor-bearing mouse model. Reproduced with permission from Ref. [55], © American Chemical Society 2019.

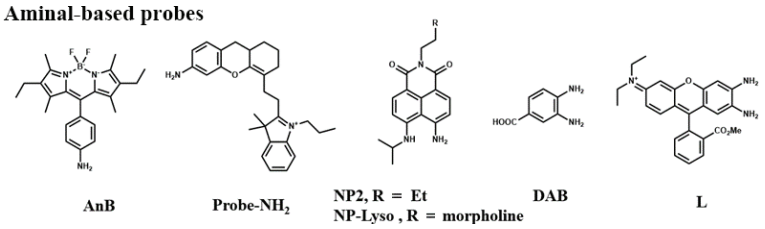

Figure 7 Chemical structure of FA probe based on aminal probes.

o-Diamines can also be used as probes for FA response sites, but since o-diamines react with methylglyoxal in living cells [61, 62], resulting in a reduced selectivity for endogenous FA, one of the amino groups is usually modified to increase the spatial site blocking effect and thus achieve enhanced specificity. Cai's group [63] used a naphthalimide derivative as a fluorophore and modified the probe NP2 with an isopropyl, which reacts with endogenous FA in live L929 cells to produce a naphthalimido-imidazole derivative, illuminating the yellow fluorescence. The first o-diamine-based fluorescent probe with endogenous FA imaging in lysosomes, NP-Lyso, was developed by attaching a morpholine group to probe NP2 as a lysosomal target [64]. Jnna's group [65] developed an ultra-simple fluorescent probe for o-diaminobenzaldehyde, 3,4-diamino benzoic acid (DAB). The probe is cheap and easy to prepare. DAB reacts with FA to give 3,4-bis(methyleneamino) benzoic acid (MABA) and 1H-benzo [d] imidazolium-6-carboxylic acid (DICA). DICA does not really emit light and MABA emits light. MABA luminescence is due to the fact that dimethylimine provides electrons for the carboxyl group on the benzene ring, which makes the molecule in the excited state, which is more conducive to the ICT interaction, resulting in fluorescence. Surprisingly, although the probe DAB does not have a modified amino group, it has low activity and no fluorescence in reaction with methylglyoxal, nitric oxide, and other bioactive compounds. In cancer cells and fibroblasts, probe DAB is able to identify both exogenous and endogenous FA. Probe L [66] has the same properties; in particular, probe L fluoresces itself purple, fluoresces red upon reaction with FA, and quenches its fluorescence upon reaction with methylglyoxal and glyoxal.

3.3 Fluorescence turn-on based on hydrazones

The formation of methylene hydrazine is facilitated by the hydrazine-FA condensation. FA has high reaction activity and small steric hindrance, which serves as the reaction foundation for the probe. Most of the hydrazine fluorescent probes take the mechanism (Fig. 8).

Lin's team developed a number of hydrazine-based FA fluorescent probes utilizing 1,8-naphthalimide as the fluorophore or backbone [67, 68], including the first hydrazine-based two-photon FA fluorophores Na-FA. The probe Na-FA reacts with FA and absorbs strongly at 543 nm. The fluorescence intensity can be increased by 900 times after FA treatment. Titration calculated the concentration range of Na-FA to be 7.1 nM, the probe Na-FA has high sensitivity, and the probe Na-FA has high selection specificity in the pH range of 5–7. Endogenous FA was found primarily in the endosome, Golgi, and lysosomes when HeLa cells had been co-cultured with probe Na-FA (Fig. 9 and Table 1). Lin's group created the first hydrazine-based lysosome-targeted FA biosensor, Na-FA-Lyso, that employs fluorophore 1,8-naphthylimine, hydrazine also as FA response site, as well as morpholine as lysosomal attacking unit. The expression level was accelerated 350-fold after treatment with 200 μM FA at a solubility of 5 for 30 min, with a concentration range of 5.02 μM. The probe exhibited strong absorption at 440 nm. Na-FA-Lyso can image endogenous FA in HaLa cells using fluorescence. His group created first endogenous FA biosensor with endoplasmic reticulum targeting for cell imaging, using p-toluenesulfonamide as endoplasmic reticulum targeting group and 1,8-naphthalimide as fluorophore. When the probe Na-FA-ER condenses with FA, it inhibits the PET pathway and lights up the fluorescence of the probe Na-FA-ER. [69]. Additionally, his team created a two-photon hydrazide fluorescent probe FA-NH_2 depending on coumarin fluorophore that can identify endogenous FA through living HaLa cells [70]. Based on 1,8-naphthalimide, Lin's team designed a first endogenous FA fluorescent probe, Nu-FA, with cell nuclear targeting [71]. HaLa cells were cultured with probe and cell dye Hoechst3342. The three-dimensional (3D) staining map of the probe has been able to get into the nucleus of HaLa cells and stain it with green fluorescence. This extends the detection of endogenous FA-induced related diseases in future clinical medicine for early screening and rehabilitation.

Yu's group [72] developed the hydrazine FA-ratio fluorescent probe CD-ND with lysosomal targeting (Fig. 10(a)) based on naphthalimide fluorophores and functionalized carbon dots, which has dual signal response properties and is capable of signal self-calibration of fluorescence intensity, enabling the fluorescent

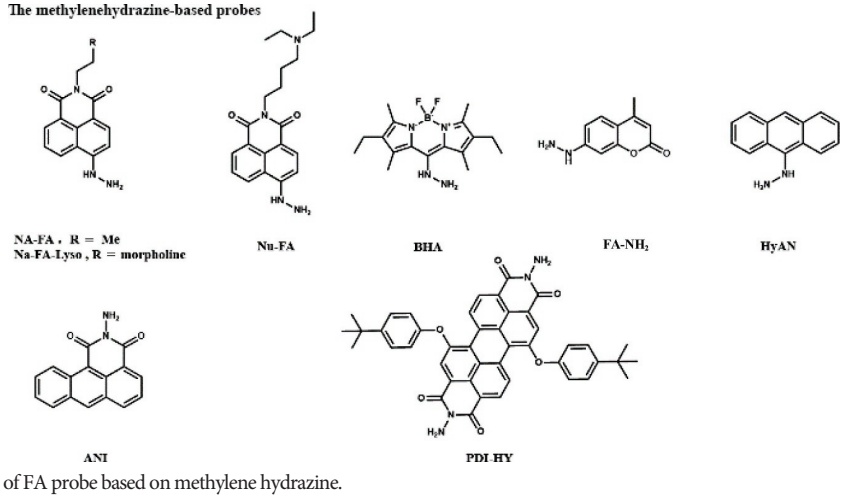

Figure 8 Chemical structure of FA probe based on methylene hydrazine.

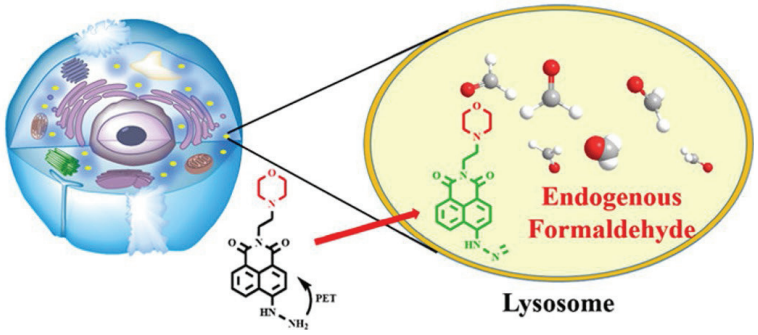

Figure 9 The response mechanism of the FA detector Na-FA fluorescent lyso. Reproduced with permission from Ref. [68], © American Chemical Society 2016.

Table 1 The distribution of FA in endoplasmic reticulum, lysosome, and Golgi apparatus was detected by Na-FA probe. Reproduced with permission from Ref. [67], © WILEY-VCH Verlag GmbH & Co. KGaA, Weinheim 2016

	Pearson's coefficient
ER-Tracker™ Red	0.6385
Lyso Tracker® Red	0.3285
Golgi-Tracker Red	0.4261
Mito Tracker® Red	0.0514

probe to exclude signal interference from non-targeting factors. Using functional fluorescent carbon dots (CDs) as the lysosomal targeting group and the fluorescent reference signal, CDs have good biocompatibility, excellent fluorescence properties, and durable optical stability [73, 74]. The emission peak of probe CD-ND at 535 nm is used as a response signal, and its signal at 414 nm is used to eliminate background interference and improve detection sensitivity. Within the same situations, the reaction mechanism of the probe CD-ND with FA conforms to the pseudo primary reaction rate equation, with a rate constant of k = 0.28 min^{-1} and a lower detection limit and shorter reaction time than the reaction mechanism of 2-aza-cope rearrangement. The low cytotoxicity of CDs reduces the cellular damage to the ND fraction, making the probe CD-ND also less cytotoxic and allowing the probe to recognize FA in living cells. The Pearson confocal correlation coefficient between blue-green fluorescence and indicator red fluorescence in HaLa cells co-cultured with CD-ND and lysosome targeting indicator was as high as 0.93, indicating that CD-ND had good lysosome targeting and imaging function. This enables the probe CD-ND to be enriched in acidic lysosomes and thus achieve lysosomal targeting properties. To investigate the endocytosis pathway of the probe, cells were treated with different endocytosis inhibitors and the experimental results showed that not only chlorpromazine but also genistein considerably lowered probe internalization, suggesting that the probe CD-ND enters the cell through the lattice-protein-mediated and niche-mediated entry. Zou et al. [75] developed a novel carbon point (rCDs) that is easy to modify the bromine substitution site and combine the carbon point with naphthalimide to construct the double emission ratio FA fluorescent probe rCDs-FA, bisulfite fluorescent probe rCD-HSO_3^-, and pH fluorescent probe rCD-pH. rCDs with blue fluorescence were prepared by a one-pot method from 2-hydrox, 1,2-diaminoethane, and 4-bromo-1,8-naphthalic anhydride. The probe rCDs-FA was obtained by a substitution reaction with hydrazine hydroxide (Fig. 10(b)). The probe rCDs-FA lit yellow-green fluorescence in response to cellular endogenous FA, which was due to the burst fluorescence of naphthamide by the probe under the action of PET, so the probe showed the blue fluorescence of citric acid; when responding with FA, the yellow-green fluorescence was produced as a result of the inhibition of PET action. The ratio fluorescence sensor virtually removes acetaldehyde and methylglyoxal interference with the probe's heterosignal, which is a novel idea for the design of FA fluorescence.

Wang's group [76] constructed a functional ratio fluorescent probe CS-OCH3@NBHN with self-assembly by grafting 4-hydrazino-1,8-naphthalimide (NBHN) and 4-methoxy-1,8-naphthalimide (MONA) on with chitosan polymer chains. Its strong hydrophilicity of the chitosan chains and hydrophobicity of the grafted MONA enabled the self-assembly in an aqueous solution. Then NBHN was also grafted onto the chitosan chains, and the nanostructure remained unchanged, resulting in nanoparticles with a diameter of 180 nm, and the FA reaction was able to maintain the nanostructure (Fig. 11). Together with the re-fluorophore NBHN and MONA, its reaction of sensor to FA inhibited the PET process of NBHN and greatly enhanced its green fluorescence, and intrinsic and extrinsic FA of HeLa cells could be imaged using the probe, CS-OCH3@NBHN.

Song's team [77] created the probe BHA based on ICT, which was obtained by replacing the chlorinated BODIPY fluorophore with a hydrazine nucleophile. When the probe BHA responds to FA, the probe molecule lights up the fluorescence in response to the ICT effect. The probe BHA is non-fluorescent, and if FA is added to the probe BHA, the fluorescent dyes are illuminated with bright blue fluorescence. The solution was colorless and transparent before the reaction and was light yellow after responding with FA. The lowest detection limit calculated by fluorescence titration measurement was 0.18 μM. The fluorescence intensity was positively correlated with pH, with increasing fluorescence intensity from pH 3 to 8, and reached the maximum fluorescence intensity at pH 8. With increasing alkalinity, a fluorescence intensity dropped dramatically from pH 8–11, reaching almost absolutely nothing by pH 11. The hydrazone reaction under alkaline conditions may generate a hydrazone salt, resulting in a fluorescence burst and a decrease in fluorescence intensity. In living HeLa cells, the probe BHA is capable of recognizing endogenous FA.

HyAN was designed by Gou's group [78] based on the optical properties of the excimer of anthracene molecule, which was prepared in one step by substituting the bromoanthracene molecule with hydrazine hydrate to obtain the probe HyAN. Because of its big aromatic conjugation planes, anthracene is frequently employed as a fluorophore in the development of molecular fluorescence detectors [79, 80]. Excimer is the term for the optical association of dimer molecules created when the lowest singlet state of two molecules collides with the ground state of the same molecule [81]. Since the probe HyAN has excellent water solubility due to hydrazine, but when it reacts with FA to form anthracene hydrazone, the water solubility decreases, which in turn self-assembles hydrophobic nanoparticles and maintains the quasimolecular state, and the quasimolecular then broadens and red-shifts the excitation spectrum, greatly enhancing the molecular

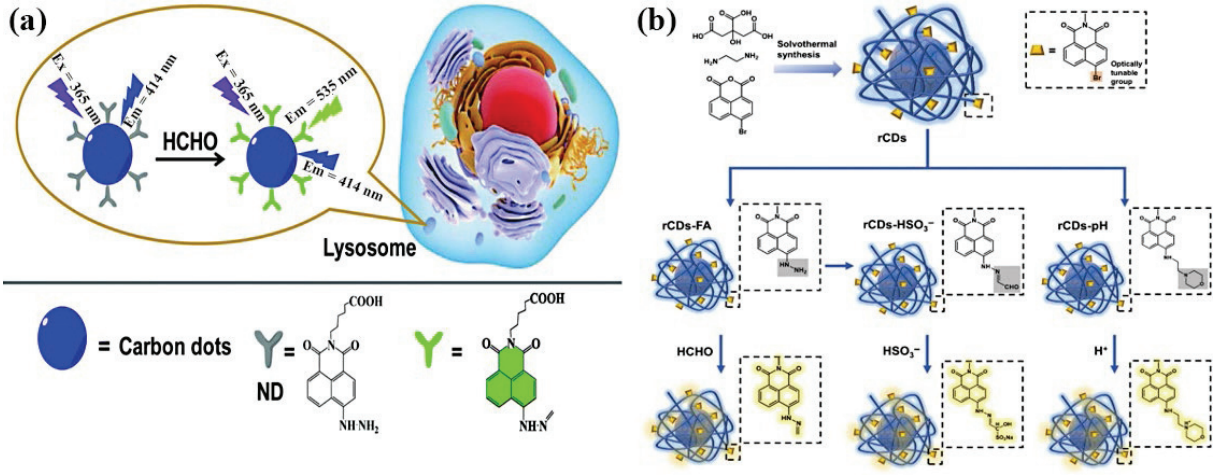

Figure 10 (a) Design of probe CD-ND and illustration of lysosome targeting imaging. Reproduced with permission from Ref. [72], © The Royal Society of Chemistry 2019. (b) The ratio fluorescence probe based on rCDs is utilized to recognize FA, bisulfite and pH. Reproduced with permission from Ref. [75], © Elsevier B.V. 2022.

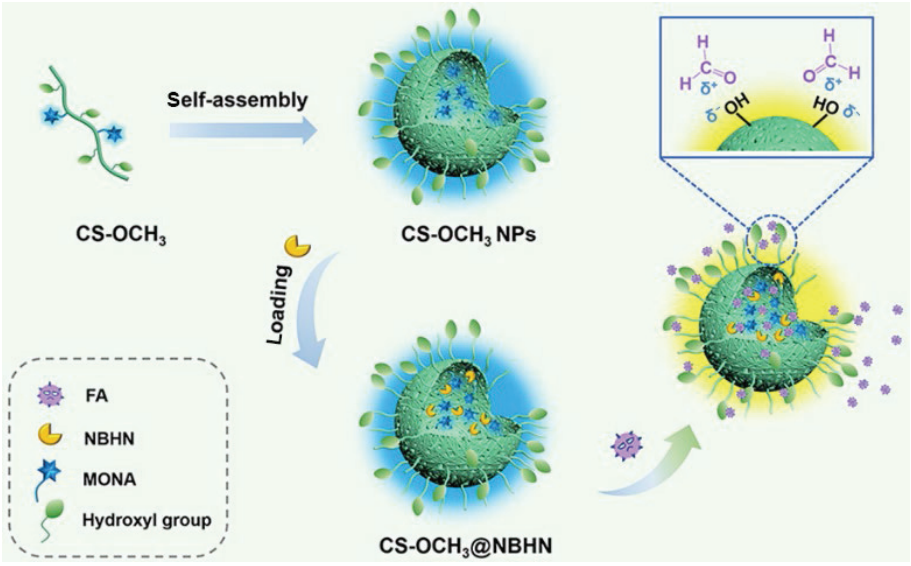

Figure 11 Design and preparation of probe CS-OCH3@NBHN. Reproduced with permission from Ref. [76], © American Chemical Society 2022.

emission and exhibiting blue fluorescence. HyAN is a probe that could identify FA in HeLa cells and L929 cells with a sensitivity of 0.23 μM.

In addition to hydrazine-based fluorescent probes, hydrazides or hydrazones can also be used as recognition units for FA to design fluorescent probes, and hydrazides contain a free amino group that responds to FA. For example, the probe ANI [82] based on N-aminoanthracene 1,9-dicarboximide reacts with FA and shows green fluorescence; the probe PDI-HY [83] uses hydrazide as the response site of FA and perylenebisimide derivative as the functional group, and the probe PDI-HY solution shows the purple color and bright yellow fluorescence after reacting with FA. However, due to the detection limit and other reasons, it is only capable of identifying exogenous FA in cells.

3.4 Other responsive turn-on fluorescent probe

New mechanisms different from the previous three types of mechanisms are referred to as other mechanisms, some new strategies also have the same high selectivity and stable optical properties to be further explored by researchers (Fig. 12).

Zhu et al. [84] discovered and demonstrated that FA cross-linked with the side chains of cysteine and lysine residues, forming a methylene bridge within the helix that allowed for a conformational change in HxIR, producing metastable activation (Fig. 13). A gene-edited FA probe, FAsor, was developed by embedding fluorescent proteins sensitive to structural changes into the HxlR specific site, enabling the expression of fluorescence in response to FA and the visualized of FA through transgenic mice nerve cells.

The R6-FA fluorescent probe was developed by Lin's team [85] using basic violet 10 as fluorophore and 1,2-diaminoethane as FA recognition site. The probe responded with FA to generate an imine intermediate, which allowed the molecule's deoxylactam to be opened to generate a ring-opened imidazole product with pink fluorescence. Capable of detecting exogenous FA in dried mushrooms and cells, Wang's group [86] developed the first regenerated FA fluorescent probe, NAP-FAP-1, using 3-(benzylamino)-succinimide as a recognition site for FA, which occurs with FA and releases FA-illuminated fluorescence after cascade reaction and burst ICT/PET dual action. The region-specific breakage of a butanimide ring's 1,5-amide bond and the benzylamine within the probe molecule provides a larger space volume for the probe, reducing side reactions such as endogenous methylglyoxal and effectively improving the selectivity of probe. Its variant NAP-FAP-2 can image endogenous FA in lysosomes. Zeng's group [87] developed the probe ABTB for imaging endogenous FA in AD mouse brain based on the ESIPT mechanism, which has regenerative FA effects. The hydroxyl group of ABTB reacts with FA to attack the carbonyl group of a five-membered heterocyclic ring, resulting in scission of the

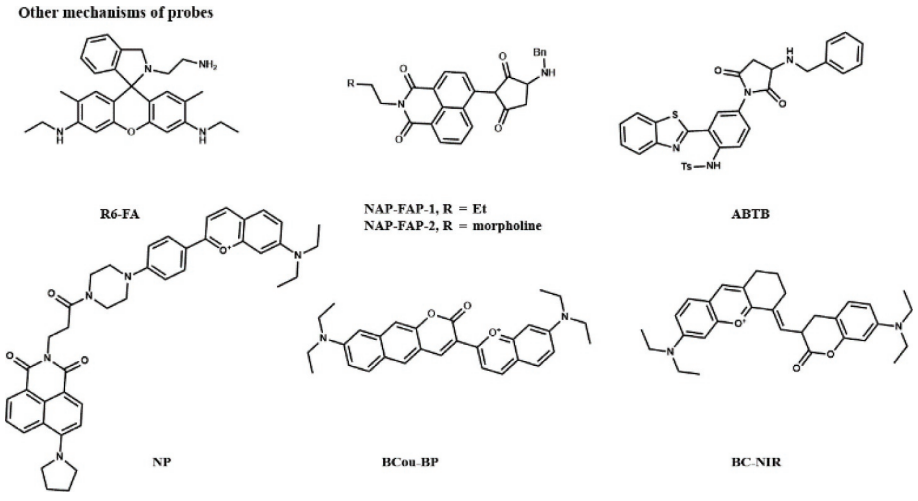

Figure 12 Chemical structure of FA probes with other mechanisms.

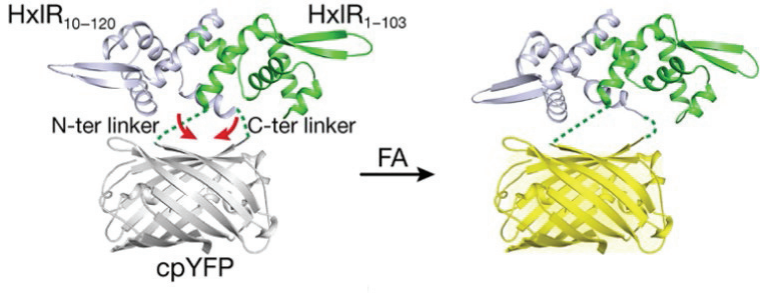

Figure 13 FAsor illuminates the fluorescence mechanism diagram. Reproduced with permission from Ref. [84], © Zhu, R. F. et al. 2021.

heterocyclic ring and the structure of a six-membered internal aliphatic ring using 3-(phenylmethylamino) pyrrolidine-2,5-dione as the reaction site. The ICT and PET effects of ABTB were broken, and the probe's fluorescence expression was inhibited. The PET effect is then suppressed, and the probe is hydrolyzed to rearrange and release the FA, thereby illuminating the fluorescence. ABTB was capable of imaging endogenous FA in AD mouse brain tissue.

FA in cells could be identified utilizing new FA/SO_2-based reversible ratio fluorescent probes; such probes carry two fluorophores with fluorescent signals in the standard state and in response to SO_2, but with different color alterations but also excitation spectra. They are able to identify and image changes in SO_2 and FA equilibrium by recording the reversible cycles of the probes' absorption spectra and color changes and converting them to absorbance. Lin's team was able to see modifications in endogenous FA and SO_2 in mice by using FA/SO_2 probes (NP) for bioimaging in the beginning (Fig. 14) [88]. By adjusting the conjugated structure of fluorophore, a fluorescent probe with mitochondrial targeting BCou-BP[89] and NIR fluorescent probes CB-NIR [90] was prepared, which can detect the dynamic changes of FA and SO_2. The FA/SO_2 reversible probe is expected to further reveal the interaction and intrinsic linkage between endogenous FA and SO_2 and to explore the potential biology and pathology of FA and SO_2 in disease studies.

4 Conclusions and outlook

On account of three chemical reactions, 2-aza-cope rearrangement reaction, condensation of $-NH_2$ and FA to form a formyl imide, and reaction of $-NHNH_2$ and FA to form hydrazone, many endogenous FA responsive turn-on probes have been constructed. This review systematically introduces the luminescence mechanisms of FA fluorescent probes, and the development process and the latest research progress of FA fluorescent probes are presented. Moreover, some novel reactions can also be applied for exploiting the FA fluorescent probes, such as 3-(benzylamino)-succinimide and 3-(phenylmethylamino) pyrrolidine-2,5-dione, which also have high selectivity and specificity for FA. These novel reactions of FA have great potential research value and need to be further optimized by researchers.

Although the FA responsive turn-on fluorescent probes have made great progress in recent years, there are still numerous challenges ahead. The probes based on amine and methylene hydrazine are simple and easy to prepare, but their selectivity falls short of the requirement of clinical application, and they may bind

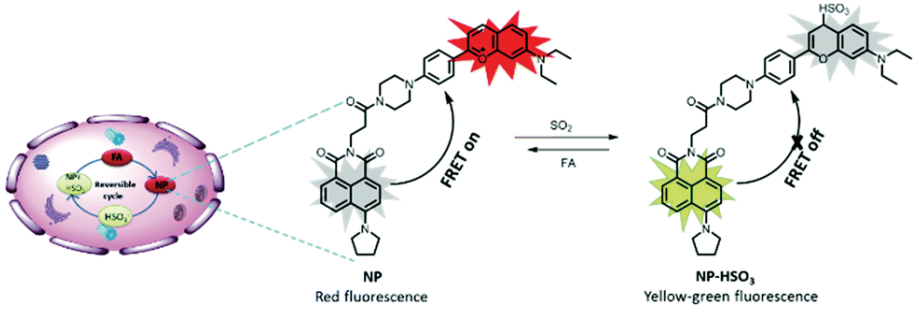

Figure 14 The probe NP's imaging strategy and mechanism. Reproduced with permission from Ref. [88], © The Royal Society of Chemistry 2019.

with acetaldehyde, methylglyoxal, and other aldehydes. Some researchers suggest that the solubility and the selectivity of the probes can be effectively improved by increasing the steric hindrance of the neighboring amino groups [91–93]. Although the selectivity and specificity of probes relying on the 2-aza-cope rearrangement are more effective, their reaction rate is not as rapid as those of imine and hydrazide probes. The 2-aza-cope rearrangement reaction mechanism has high selectivity and specificity for formaldehyde, so it can be used to construct formaldehyde fluorescent probes without interference from active carbonyl compounds in the organism. 2-Aza-cope rearrangement is a fast response that can achieve rapid response and real-time monitoring. Disadvantages of FA fluorescent probes based on $-NH_2$ and $-NHNH_2$ include: (1) Lack of selectivity and specificity: These probes have low selectivity and specificity for FA, making them vulnerable to interference from other reactive amine compounds, which may result in false positives or negatives. (2) Low detection sensitivity: Compared with probes based on 2-aza-cope rearrangement reaction, those based on $-NH_2$ and $-NHNH_2$ have lower detection sensitivity and may not be able to detect low concentrations of FA. (3) Susceptibility to biological environments: These probes are sensitive to the biological environment and may lead to interference or suppression of the fluorescent signal, affecting the detection results. (4) High complexity: Synthesis and handling of probes based on $-NH_2$ and $-NHNH_2$ are complex, which makes them difficult to use for rapid detection and application. Another challenge is that fewer FA fluorescent probes can penetrate tissues deeply for imaging, whereas NIR fluorescent probes have superior photochemical imaging advantages with enormous potential in clinical translation (Table 2). The trends of FA fluorescent probes include: (1) low detection limits and short response times for acquiring better real-time performance; (2) high selectivity with inertness to other endogenous aldehyde compounds; (3) low cytotoxicity with biocompatibility; and (4) deep tissue imaging with new fluorescent turn-on mechanisms. It is noted that the construction of FA fluorescent probes with multifunctional cascade responses can enable targeted imaging, which improves the efficiency of disease detection. In addition, the two-photon fluorescent probes with ratiometric imaging [94] can successfully reduce light loss and their own fluorescence background, as well as improve the spatial resolution [95].

In the past two years, Jiang's group [96] developed a probe RBNA, which can detect exogenous FA in zebrafish, reflect the freshness of seafood products, and provide a useful tool for simple detection of seafood safety. Li's team [97] developed a near-infrared probe Probe-$NHNH_2$ capable of *in situ* imaging of THF-induced FA after 10 min. Liu's team [98] developed an endogenous FA imaging probe NP-FA that can cross the blood–brain barrier in mice with Alzheimer's disease and has endoplasmic reticulum targeting, which provides a new opportunity to reveal the inherent pathological relationship between FA and Alzheimer's disease and to diagnose and treat it. At present, there are few FA probes that can be used *in vivo*, which are restricted by the following aspects: (1) weak targeting, most of the existing FA probes are small molecular probes, which cannot target proteins and do not have stable targeting; (2) short residence time, small molecular probes exist as single molecules in the body, so they are easy to be excluded and absorbed by organisms, and cannot be detained in tumor cells for a long time; and (3) the penetration of fluorescence below 650 nm is weak. In order to obtain good imaging effect *in vivo*, it is necessary for the probe to emit fluorescence from the first and second regions of the near infrared in order to reduce the influence of light astigmatism and absorption of skin tissue. In the future, researchers can focus on the research and development of assembled fluorescent probes of quantum dots, proteins, and peptides, which can effectively improve their retention time and targeting ability *in vivo*, and are

Table 2 Fluorescent probes for FA imaging *in vitro* and *in vivo*

Probe	Luminescence mechanism	Reaction mechanism	Limit of detection (LOD)	Ex/Em (nm)	Application	Ref.
FP1	PET	2-Aza-cope	10 μM	633/649	Endogenous FA	[46]
FAP-1	PET	2-Aza-cope	5 mM	645/662	Endogenous FA	[47]
FATP-1	ICT	2-Aza-cope	0.3 μM	371/571	Endogenous FA	[51]
FFP706	PET	2-Aza-cope	2.5 μM	670/706	Live mice	[53]
EGFP	Fluorescent protein	2-Aza-cope	25 μM	468/510	Endogenous FA	[54]
Ru-FA	PET	2-Aza-cope	0.02 μM	460/634	Endogenous FA	[55]
FormAFP	ESIPT	2-Aza-cope	0.06 μM	340/520	Oxidative stress stimulation	[57]
AnB	PET	Aminal	0.16 μM	520/535	Exogenous FA	[58]
Probe-NH_2	PET	Aminal	1.87 μM	670/706	Live mice	[59]
NP2	ICT	Aminal	1.8 μM	380/450	Endogenous FA	[63]
DAB	ICT	Aminal	0.12 μM	345/430	Endogenous FA	[65]
Na-FA	PET	Hydrazine	0.71 μM	440/543	Endogenous FA	[67]
FA-NH_2	PET	Hydrazine	0.06 μM	370/670	Endogenous FA	[70]
CD-ND	PET	Hydrazine	0.34 μM	365/535	Endogenous FA	[72]
CS-OCH_3@NBHN	PET	Hydrazine	0.66 μM	405/545	Endogenous FA	[76]
BHA	ICT	Hydrazine	0.18 μM	499/514	Endogenous FA	[77]
HyAN	Excimer	Hydrazine	0.23 μM	258/445	Endogenous FA	[78]
ANI	PET	Hydrazine	0.99 μM	440/518	Exogenous FA	[82]
PDI-HY	PET	Hydrazine	1.5 μM	450/582	Exogenous FA	[83]
R6-FA	PET	Ethylenediamine	0.77 μM	530/560	Exogenous FA	[85]
NAP-FAP-1	ICT/PET	3-(Benzylamino)-succinimide	0.48 μM	359/470	Endogenous FA	[86]

more controllable and stable for fluorescence emission. Its selectivity or affinity to the substrate can be adjusted to adjust its optical properties. Any modification of the binding site of the small molecular probe may lead to the change of the emission performance of the molecule, which is not easy to be modified and optimized.

As a result, the fluorescence turn-on approach has wide applicability for sensing endogenous FA. The intricate inherent connections between biology and pathology of endogenous FA will be revealed by the improvement of FA responsive fluorescent probes. Similarly, FA responsive fluorescent probes will be helpful in the treatment of illnesses such as Fanconi anemia and Alzheimer's disease in the future, as well as in the early detection of cancer in clinical settings.

Acknowledgments

This work was financially supported by the National Natural Science Foundation of China (No. 52173138), Natural Science Foundation of Hubei Province (No. 2021CFB298), and Natural Science Foundation of Shandong Province (No. ZR2021ME015).

References

[1] Lai, Y. Q.; Yu, R.; Hartwell, H. J.; Moeller, B. C.; Bodnar, W. M.; Swenberg, J. A. Measurement of endogenous versus exogenous formaldehyde-induced DNA-protein crosslinks in animal tissues by stable isotope labeling and ultrasensitive mass spectrometry. *Cancer Res.* **2016**, *76*, 2652–2661.

[2] Kou, Y. D.; Zhao, H.; Cui, D. H.; Han, H. B.; Tong, Z. Q. Formaldehyde toxicity in age-related neurological dementia. *Ageing Res. Rev.* **2022**, *73*, 101512.

[3] Wolkoff, P. Indoor air pollutants in office environments: Assessment of comfort, health, and performance. *Int. J. Hyg. Environ. Health* **2013**, *216*, 371–394.

[4] Morellato, A. E.; Umansky, C.; Pontel, L. B. The toxic side of one-carbon metabolism and epigenetics. *Redox Biol.* **2021**, *40*, 101850.

[5] Vasilyev, N.; Williams, T.; Brennan, M. L.; Unzek, S.; Zhou, X. R.; Heinecke, J. W.; Spitz, D. R.; Topol, E. J.; Hazen, S. L.; Penn, M. S. Myeloperoxidase-generated oxidants modulate left ventricular remodeling but not infarct size after myocardial infarction. *Circulation* **2005**, *112*, 2812–2820.

[6] Burgos-Barragan, G.; Wit, N.; Meiser, J.; Dingler, F. A.; Pietzke, M.; Mulderrig, L.; Pontel, L. B.; Rosado, I. V.; Brewer, T. F.; Cordell, R. L. et al. Mammals divert endogenous genotoxic formaldehyde into one-carbon metabolism. *Nature* **2017**, *548*, 549–554.

[7] Umansky, C.; Morellato, A. E.; Rieckher, M.; Scheidegger, M. A.; Martinefski, M. R.; Fernández, G. A.; Pak, O.; Kolesnikova, K.; Reingruber, H.; Bollini, M. et al. Endogenous formaldehyde scavenges cellular glutathione resulting in redox disruption and cytotoxicity. *Nat. Commun.* **2022**, *13*, 745.

[8] Swenberg, J. A.; Moeller, B. C.; Lu, K.; Rager, J. E.; Fry, R. C.; Starr, T. B. Formaldehyde carcinogenicity research: 30 years and counting for mode of action, epidemiology, and cancer risk assessment. *Toxicol. Pathol.* **2013**, *41*, 181–189.

[9] Chen, N. H.; Djoko, K. Y.; Veyrier, F. J.; McEwan, A. G. Formaldehyde stress responses in bacterial pathogens. *Front. Microbiol.* **2016**, *7*, 257.

[10] Jung, M.; Smogorzewska, A. Hematopoiesis and stem cells: Endogenous formaldehyde destroys blood stem cells. *Blood* **2021**, *137*, 1988–1990.

[11] Rohlhill, J.; Har, J. R. G.; Antoniewicz, M. R.; Papoutsakis, E. T. Improving synthetic methylotrophy via dynamic formaldehyde regulation of pentose phosphate pathway genes and redox perturbation. *Metab. Eng.* **2020**, *57*, 247–255.

[12] Lu, K.; Craft, S.; Nakamura, J.; Moeller, B. C.; Swenberg, J. A. Use of LC-MS/MS and stable isotopes to differentiate hydroxymethyl and methyl DNA adducts from formaldehyde and nitrosodimethylamine. *Chem. Res. Toxicol.* **2012**, *25*, 664–675.

[13] Ma, B. K.; Xu, F. J.; He, M.; Lin, Y. Q.; Hu, G. H.; Zhang, M.; Zhao, X. Y.; Liu, W. L. Detection of residual formaldehyde in N-butyl-2-cyanoacrylate by high-performance liquid chromatography with rhodamine B hydrazide. *Microchem. J.* **2020**, *158*, 105222.

[14] Cordis, G. A.; Bagchi, D.; Maulik, N.; Das, D. K. High-performance liquid chromatographic method for the simultaneous detection of malonaldehyde, acetaldehyde, formaldehyde, acetone and propionaldehyde to monitor the oxidative stress in heart. *J. Chromatogr. A* **1994**, *661*, 181–191.

[15] Silva, A. F. S.; Goncalves, I. C.; Rocha, F. R. P. Smartphone-based digital images as a novel approach to determine formaldehyde as a milk adulterant. *Food Control* **2021**, *125*, 107956.

[16] Wongniramaikul, W.; Limsakul, W.; Choodum, A. A biodegradable colorimetric film for rapid low-cost field determination of formaldehyde contamination by digital image colorimetry. *Food Chem.* **2018**, *249*, 154–161.

[17] Bianchi, F.; Careri, M.; Musci, M.; Mangia, A. Fish and food safety: Determination of formaldehyde in 12 fish species by SPME extraction and GC-MS analysis. *Food Chem.* **2007**, *100*, 1049–1053.

[18] Oancea, A.; Hanoune, B.; Focsa, C.; Chazallon, B. Cross determination of the vapor liquid equilibrium of formaldehyde aqueous solutions by quadrupole mass spectrometry and infrared diode laser spectroscopy. *Environ. Sci. Technol.* **2009**, *43*, 435–440.

[19] Lipari, F.; Swarin, S. J. 2, 4-Dinitrophenylhydrazine-coated Florisil sampling cartridges for the determination of formaldehyde in air. Environ. Sci. *Technol.* **1985**, *19*, 70–74.

[20] Bruemmer, K. J.; Brewer, T. F.; Chang, C. J. Fluorescent probes for imaging formaldehyde in biological systems. *Curr. Opin. Chem. Biol.* **2017**, *39*, 17–23.

[21] Liu, X.; Li, N.; Li, M.; Chen, H.; Zhang, N. N.; Wang, Y. L.; Zheng, K. B. Recent progress in fluorescent probes for detection of carbonyl species: Formaldehyde, carbon monoxide and phosgene. *Coord. Chem. Rev.* **2020**, *404*, 213109.

[22] Kumaravel, S.; Wu, S. H.; Chen, G. Z.; Huang, S. T.; Lin, C. M.; Lee, Y. C.; Chen, C. H. Development of ratiometric electrochemical molecular switches to assay endogenous formaldehyde in live cells, whole blood and creatinine in saliva. *Biosens. Bioelectron.* **2021**, *171*, 112720.

[23] Hämmerle, M.; Hall, E. A. H.; Cade, N.; Hodgins, D. Electrochemical enzyme sensor for formaldehyde operating in the gas phase. *Biosens. Bioelectron.* **1996**, *11*, 239–246.

[24] Sandler, S.; Strom, R. Determination of formaldehyde by gas chromatography. *Anal. Chem.* **1960**, *32*, 1890–1891.

[25] Zhao, X. J.; Ji, C. D.; Ma, L.; Wu, Z.; Cheng, W. Y.; Yin, M. Z. An aggregation-induced emission-based "turn-on" fluorescent probe for facile detection of gaseous formaldehyde. *ACS Sens.* **2018**, *3*, 2112–2117.

[26] Sun, X. X.; Zhang, H.; Hao, S.; Zhai, J. F.; Dong, S. J. A self-powered biosensor with a flake electrochromic display for electrochemical and colorimetric formaldehyde detection. *ACS Sens.* **2019**, *4*, 2631–2637.

[27] Escudero, D. Revising intramolecular photoinduced electron transfer (PET) from first-principles. *Acc. Chem. Res.* **2016**, *49*, 1816–1824.

[28] Bauer, A.; Westkämper, F.; Grimme, S.; Bach, T. Catalytic enantioselective reactions driven by photoinduced electron transfer. *Nature* **2005**, *436*, 1139–1140.

[29] Dadashi-Silab, S.; Doran, S.; Yagci, Y. Photoinduced electron transfer reactions for macromolecular syntheses. *Chem. Rev.* **2016**, *116*, 10212–10275.

[30] Allen, A. R.; Noten, E. A.; Stephenson, C. R. Aryl transfer strategies mediated by photoinduced electron transfer. *Chem. Rev.* **2022**, *122*, 2695–2751.

[31] Gui, B.; Meng, Y.; Xie, Y.; Tian, J. W.; Yu, G.; Zeng, W. X.; Zhang, G. X.; Gong, S. L.; Yang, C. L.; Zhang, D. Q. et al. Tuning the photoinduced electron transfer in a Zr-MOF: Toward solid-state fluorescent molecular switch and turn-on sensor. *Adv. Mater.* **2018**, *30*, 1802329.

[32] Yoshihara, T.; Druzhinin, S. I.; Zachariasse, K. A. Fast intramolecular charge transfer with a planar rigidized electron donor/acceptor molecule. *J. Am. Chem. Soc.* **2004**, *126*, 8535–8539.

[33] Wang, C.; Qiao, Q. L.; Chi, W. J.; Chen, J.; Liu, W. J.; Tan, D.;

McKechnie, S.; Lyu, D.; Jiang, X. F.; Zhou, W. et al. Quantitative design of bright fluorophores and AIEgens by the accurate prediction of twisted intramolecular charge transfer (TICT). *Angew. Chem.* **2020**, *132*, 10246–10258.

[34] Qian, F.; Zhang, C. L.; Zhang, Y. M.; He, W. J.; Gao, X.; Hu, P.; Guo, Z. J. Visible light excitable Zn^{2+} fluorescent sensor derived from an intramolecular charge transfer fluorophore and its *in vitro* and *in vivo* application. *J. Am. Chem. Soc.* **2009**, *131*, 1460–1468.

[35] Sedgwick, A. C.; Wu, L. L.; Han, H. H.; Bull, S. D.; He, X. P.; James, T. D.; Sessler, J. L.; Tang, B. Z.; Tian, H.; Yoon, J. Excited-state intramolecular proton-transfer (ESIPT) based fluorescence sensors and imaging agents. *Chem. Soc. Rev.* **2018**, *47*, 8842–8880.

[36] Jiang, G. W.; Jin, Y.; Li, M.; Wang, H. L.; Xiong, M. Y.; Zeng, W. L.; Yuan, H.; Liu, C. L.; Ren, Z. Q.; Liu, C. R. Faster and more specific: Excited-state intramolecular proton transfer-based dyes for high-fidelity dynamic imaging of lipid droplets within cells and tissues. *Anal. Chem.* **2020**, *92*, 10342–10349.

[37] Seo, J.; Kim, S.; Park, S. Y. Strong solvatochromic fluorescence from the intramolecular charge-transfer state created by excited-state intramolecular proton transfer. *J. Am. Chem. Soc.* **2004**, *126*, 11154–11155.

[38] Li, Y. H.; Dahal, D.; Abeywickrama, C. S.; Pang, Y. Progress in tuning emission of the excited-state intramolecular proton transfer (ESIPT)-based fluorescent probes. *ACS Omega* **2021**, *6*, 6547–6553.

[39] Clegg, R. M. Fluorescence resonance energy transfer. *Curr. Opin. Biotechnol.* **1995**, *6*, 103–110.

[40] Miao, Y. W.; Sathiyan, G.; Wang, H. X.; Tian, Y.; Chen, C.; Ding, X. D.; Zhai, M. D.; Yang, X. C.; Cheng, M. Construction of efficient perovskite solar cell through small-molecule synergistically assisted surface defect passivation and fluorescence resonance energy transfer. *Chem. Eng. J.* **2021**, *426*, 131358.

[41] Wu, Y.; Yan, C. X.; Li, X. S.; You, L. H.; Yu, Z. Q.; Wu, X. F.; Zheng, Z. G.; Liu, G. F.; Guo, Z. Q.; Tian, H. et al. Circularly polarized fluorescence resonance energy transfer (*C*-FRET) for efficient chirality transmission within an intermolecular system. *Angew. Chem.* **2021**, *133*, 24754–24762.

[42] Li, Y. B.; Wang, L.; Zhao, L. T.; Li, M.; Wen, Y. M. An fluorescence resonance energy transfer sensing platform based on signal amplification strategy of hybridization chain reaction and triplex DNA for the detection of Chloramphenicol in milk. *Food Chem.* **2021**, *357*, 129769.

[43] Wu, J. S.; Liu, W. M.; Ge, J. C.; Zhang, H. Y.; Wang, P. F. New sensing mechanisms for design of fluorescent chemosensors emerging in recent years. *Chem. Soc. Rev.* **2011**, *40*, 3483–3495.

[44] Goodman, C. G.; Johnson, J. S. Asymmetric synthesis of β-amino amides by catalytic enantioconvergent 2-aza-cope rearrangement. *J. Am. Chem. Soc.* **2015**, *137*, 14574–14577.

[45] Wei, L.; Chang, X.; Wang, C. J. Catalytic asymmetric reactions with N-metallated azomethine ylides. *Acc. Chem. Res.* **2020**, *53*, 1084–1100.

[46] Roth, A.; Li, H.; Anorma, C.; Chan, J. A reaction-based fluorescent probe for imaging of formaldehyde in living cells. *J. Am. Chem. Soc.* **2015**, *137*, 10890–10893.

[47] Brewer, T. F.; Chang, C. J. An aza-cope reactivity-based fluorescent probe for imaging formaldehyde in living cells. *J. Am. Chem. Soc.* **2015**, *137*, 10886–10889.

[48] Lee, M. G.; Wynder, C.; Schmidt, D. M.; McCafferty, D. G.; Shiekhattar, R. Histone H3 lysine 4 demethylation is a target of nonselective antidepressive medications. *Chem. Biol.* **2006**, *13*, 563–567.

[49] Liu, J.; Liu, F. Y.; Tong, Z. Q.; Li, Z. H.; Chen, W.; Luo, W. H.; Li, H.; Luo, H. J.; Tang, Y.; Tang, J. M. et al. Lysine-specific demethylase 1 in breast cancer cells contributes to the production of endogenous formaldehyde in the metastatic bone cancer pain model of rats. *PLoS One* **2013**, *8*, e58957.

[50] Stazi, G.; Zwergel, C.; Valente, S.; Mai, A. LSD1 inhibitors: A patent review (2010–2015). *Expert Opin. Ther. Pat.* **2016**, *26*, 565–580.

[51] Chen, J.; Shao, C. W.; Wang, X. A.; Gu, J.; Zhu, H. L.; Qian, Y. Imaging of formaldehyde fluxes in epileptic brains with a two-photon fluorescence probe. *Chem. Commun.* **2020**, *56*, 3871–3874.

[52] Vu, H. T.; Akatsu, H.; Hashizume, Y.; Setou, M.; Ikegami, K. Increase in α-tubulin modifications in the neuronal processes of hippocampal neurons in both kainic acid-induced epileptic seizure and Alzheimer's disease. *Sci. Rep.* **2017**, *7*, 40205.

[53] Du, Y. M.; Zhang, Y. Q.; Huang, M. R.; Wang, S. S.; Wang, J. Z.; Liao, K. K.; Wu, X. J.; Zhou, Q.; Zhang, X. H.; Wu, Y. D. et al. Systematic investigation of the aza-cope reaction for fluorescence imaging of formaldehyde *in vitro* and *in vivo*. *Chem. Sci.* **2021**, *12*, 13857–13869.

[54] Zhang, Y. Q.; Du, Y. M.; Li, M. J.; Zhang, D.; Xiang, Z.; Peng, T. Activity-based genetically encoded fluorescent and luminescent probes for detecting formaldehyde in living cells. *Angew. Chem.* **2020**, *132*, 16494–16498.

[55] Liu, C. L.; Zhang, R.; Zhang, W. Z.; Liu, J. P.; Wang, Y. L.; Du, Z. B.; Song, B.; Xu, Z. P.; Yuan, J. L. "Dual-key-and-lock" ruthenium complex probe for lysosomal formaldehyde in cancer cells and tumors. J. Am. *Chem. Soc.* **2019**, *141*, 8462–8472.

[56] Mindell, J. A. Lysosomal acidification mechanisms. *Annu. Rev. Physiol.* **2012**, *74*, 69–86.

[57] Quan, T. T.; Liang, Z. H.; Pang, H. T.; Zeng, G. L.; Chen, T. S. A ratiometric ESIPT probe based on 2-aza-cope rearrangement for rapid and selective detection of formaldehyde in living cells. *Analyst* **2022**, *147*, 252–261.

[58] Song, H.; Rajendiran, S.; Kim, N.; Jeong, S. K.; Koo, E.; Park, G.; Thangadurai, T. D.; Yoon, S. A tailor designed fluorescent "turn-on" sensor of formaldehyde based on the BODIPY motif. *Tetrahedron Lett.* **2012**, *53*, 4913–4916.

[59] Ding, N.; Li, Z.; Hao, Y. T.; Yang, X. B. A new amine moiety-based near-infrared fluorescence probe for detection of formaldehyde in real food samples and mice. *Food Chem.* **2022**, *384*, 132426.

[60] He, X. Y.; Hu, Y. M.; Shi, W.; Li, X. H.; Ma, H. M. Design, synthesis and application of a near-infrared fluorescent probe for *in vivo* imaging of aminopeptidase N. *Chem. Commun.* **2017**, *53*, 9438–9441.

[61] Wang, T. N.; Douglass Jr, E. F.; Fitzgerald, K. J.; Spiegel, D. A. A "turn-on" fluorescent sensor for methylglyoxal. *J. Am. Chem. Soc.* **2013**, *135*, 12429–12433.

[62] Wang, W. L.; Chen, J. L.; Ma, H. J.; Xing, W. J.; Lv, N.; Zhang, B. N.; Xu, H.; Wang, W.; Lou, K. Y. An "AND"-logic-gate-based fluorescent probe with dual reactive sites for monitoring extracellular methylglyoxal level changes of activated macrophages. *Chem. Commun.* **2021**, *57*, 8166–8169.

[63] Cai, S. T.; Liu, C.; Jiao, X. J.; Zhao, L. C.; Zeng, X. S. A rational design of fluorescent probes for specific detection and imaging of endogenous formaldehyde in living cells. *Tetrahedron* **2020**, *76*, 131617.

[64] Cai, S. T.; Liu, C.; Gong, J.; He, S.; Zhao, L. C.; Zeng, X. S. A lysosome-targeted fluorescent probe for the specific detection and imaging of formaldehyde in living cells. *Spectrochim. Acta Part A* **2021**, *245*, 118949.

[65] Jana, A.; Joseph, M. M.; Munan, S.; Shamna, K.; Maiti, K. K.; Samanta, A. A single benzene fluorescent probe for efficient formaldehyde sensing in living cells using glutathione as an amplifier. *J. Photochem. Photobiol. B* **2021**, *214*, 112091.

[66] Liu, C.; Jiao, X. J.; He, S.; Zhao, L. C.; Zeng, X. S. A reaction-based fluorescent probe for the selective detection of formaldehyde and methylglyoxal via distinct emission patterns. *Dyes Pigm.* **2017**, *138*, 23–29.

[67] Tang, Y. H.; Kong, X. Q.; Xu, A.; Dong, B. L.; Lin, W. Y. Development of a two-photon fluorescent probe for imaging of endogenous formaldehyde in living tissues. *Angew. Chem.* **2016**, *55*, 3356–3359.

[68] Tang, Y. H.; Kong, X. Q.; Liu, Z. R.; Xu, A.; Lin, W. Y. Lysosome-targeted turn-on fluorescent probe for endogenous formaldehyde in living cells. *Anal. Chem.* **2016**, *88*, 9359–9363.

[69] Tang, Y. H.; Ma, Y. Y.; Xu, A.; Xu, G. P.; Lin, W. Y. A turn-on fluorescent probe for endogenous formaldehyde in the endoplasmic reticulum of living cells. *Methods Appl. Fluoresc.* **2017**, *5*, 024005.

[70] Zhang, Y. B.; Qiu, X. Y.; Sun, L.; Yan, Q.; Luck, R. L.; Liu, H. Y. A two-photon fluorogenic probe based on a coumarin schiff base for

formaldehyde detection in living cells. *Spectrochim. Acta Part A* **2022**, *274*, 121074.
[71] Li, J. F.; Ding, D. H.; Song, W. H.; Wang, J. Y.; Quan, W.; Huang, L.; Lin, W. Y. Visualization of endogenous formaldehyde in the nucleus via a robust activatable fluorescent probe. *Sens. Actuators B* **2022**, *368*, 132136.
[72] Chen, S.; Jia, Y.; Zou, G. Y.; Yu, Y. L.; Wang, J. H. A ratiometric fluorescent nanoprobe based on naphthalimide derivative-functionalized carbon dots for imaging lysosomal formaldehyde in HeLa cells. *Nanoscale* **2019**, *11*, 6377–6383.
[73] Shuang, E.; Mao, Q. X.; Yuan, X. L.; Kong, X. L.; Chen, X. W.; Wang, J. H. Targeted imaging of the lysosome and endoplasmic reticulum and their pH monitoring with surface regulated carbon dots. *Nanoscale* **2018**, *10*, 12788–12796.
[74] Hua, X. W.; Bao, Y. W.; Wu, F. G. Fluorescent carbon quantum dots with intrinsic nucleolus-targeting capability for nucleolus imaging and enhanced cytosolic and nuclear drug delivery. *ACS Appl. Mater. Interfaces* **2018**, *10*, 10664–10677.
[75] Zou, G. Y.; Guo, L.; Chen, S.; Liu, N. Z.; Yu, Y. L. Multifunctional ratiometric fluorescent sensing platform constructed by grafting various response groups on carbon dots with bromine active site for biosensing and bioimaging. *Sens. Actuators B* **2022**, *357*, 131376.
[76] Yang, L. N.; Han, Q. X.; Ling, X. L.; Wang, Y. S.; Li, M. H.; Chen, Q. L.; Wang, X. C. N-butyl-4-hydrazino-1,8-naphthalimide-loaded chitosan self-assembled nanoparticles as fluorescent ratiometric chemosensors for detection of formaldehyde. *ACS Appl. Nano Mater.* **2022**, *5*, 7392–7401.
[77] Chen, H. W.; Li, H.; Song, Q. H. BODIPY-substituted hydrazine as a fluorescent probe for rapid and sensitive detection of formaldehyde in aqueous solutions and in live cells. *ACS Omega* **2018**, *3*, 18189–18195.
[78] Han, B. C.; Sun, J.; Chen, K.; Chen, Z. Y.; Huang, M. H.; Gao, Z. Z.; Hou, X. F. A novel fluorescent probe for formaldehyde based-on monomer–excimer conversion and its imaging in live cells. *Tetrahedron* **2018**, *74*, 7193–7197.
[79] Kaanumalle, L. S.; Gibb, C. L. D.; Gibb, B. C.; Ramamurthy, V. A hydrophobic nanocapsule controls the photophysics of aromatic molecules by suppressing their favored solution pathways. *J. Am. Chem. Soc.* **2005**, *127*, 3674–3675.
[80] Das, A.; Danao, A.; Banerjee, S.; Raj, A. M.; Sharma, G.; Prabhakar, R.; Srinivasan, V.; Ramamurthy, V.; Sen, P. Dynamics of anthracene excimer formation within a water-soluble nanocavity at room temperature. *J. Am. Chem. Soc.* **2021**, *143*, 2025–2036.
[81] Karuppannan, S.; Chambron, J. C. Supramolecular chemical sensors based on pyrene monomer–excimer dual luminescence. *Chem. Asian J.* **2011**, *6*, 964–984.
[82] Wu, F.; Zhang, Y.; Huang, L.; Xu, D.; Wang, H. Y. A fluorescence-enhanced probe for rapid detection of formaldehyde and its application for cell imaging. *Anal. Methods* **2017**, *9*, 5472–5477.
[83] Cheng, H. R.; Zou, L. W.; Yang, L.; Wang, Z. G.; Lu, X. J. A turn-on fluorescence probe for rapid, sensitive and visual detection of formaldehyde. *ChemistrySelect* **2019**, *4*, 432–436.
[84] Zhu, R. F.; Zhang, G.; Jing, M.; Han, Y.; Li, J. F.; Zhao, J. Y.; Li, Y. L.; Chen, P. R. Genetically encoded formaldehyde sensors inspired by a protein intra-helical crosslinking reaction. *Nat. Commun.* **2021**, *12*, 581.
[85] He, L. W.; Yang, X. L.; Ren, M. G.; Kong, X. Q.; Liu, Y.; Lin, W. Y. An ultra-fast illuminating fluorescent probe for monitoring formaldehyde in living cells, shiitake mushrooms, and indoors. *Chem. Commun.* **2016**, *52*, 9582–9585.
[86] Xu, H.; Xu, H.; Ma, S. N.; Chen, X. N.; Huang, L. X.; Chen, J. W.; Gao, F.; Wang, R.; Lou, K. Y.; Wang, W. Analyte regeneration fluorescent probes for formaldehyde enabled by regiospecific formaldehyde-induced intramolecularity. *J. Am. Chem. Soc.* **2018**, *140*, 16408–16412.
[87] Bi, A. Y.; Liu, M.; Huang, S.; Zheng, F.; Ding, J. P.; Wu, J. Y.; Tang, G.; Zeng, W. B. Construction and theoretical insights into the ESIPT fluorescent probe for imaging formaldehyde *in vitro* and *in vivo*. *Chem. Commun.* **2021**, *57*, 3496–3499.
[88] Ma, Y. Y.; Gao, W. J.; Zhu, L. L.; Zhao, Y. P.; Lin, W. Y. Development of a unique reversible fluorescent probe for tracking endogenous sulfur dioxide and formaldehyde fluctuation *in vivo*. *Chem. Commun.* **2019**, *55*, 11263–11266.
[89] Wang, M. Z.; Liu, Q. L.; Sun, X.; Zheng, S.; Ma, Y. Y.; Wang, Y.; Yan, M.; Lu, Z. L.; Fan, C. H.; Lin, W. Y. Ratiometric and reversible detection of endogenous SO_2 and HCHO in living cells and mice by a near-infrared and dual-emission fluorescent probe. *Sens. Actuators B* **2021**, *335*, 129649.
[90] Zhu, H. C.; Zhang, X.; Liu, C. Y.; Zhang, Y.; Su, M. J.; Rong, X. D.; Wang, X.; Liu, M. Y.; Zhang, X. H.; Sheng, W. L. et al. A reversible NIR fluorescent probe for monitoring of SO_2 and formaldehyde in live cells and zebrafish. *Sens. Actuators B* **2022**, *366*, 131962.
[91] Tang, Y. H.; Ma, Y. Y.; Yin, J. L.; Lin, W. Y. Strategies for designing organic fluorescent probes for biological imaging of reactive carbonyl species. *Chem. Soc. Rev.* **2019**, *48*, 4036–4048.
[92] Sun, Y. Q.; Sun, P. J.; Li, Z. H.; Qu, L. H.; Guo, W. Natural flavylium-inspired far-red to NIR-II dyes and their applications as fluorescent probes for biomedical sensing. *Chem. Soc. Rev.* **2022**, *51*, 7170–7205.
[93] Huang, S. M.; Li, Z. J.; Liu, M. H.; Zhou, M. J.; Weng, J. T.; He, Y.; Jiang, Y.; Zhang, H. T.; Sun, H. Y. Reaction-based fluorescent and chemiluminescent probes for formaldehyde detection and imaging. *Chem. Commun.* **2022**, *58*, 1442–1453.
[94] Yao, S.; Belfield, K. D. Two-photon fluorescent probes for bioimaging. *Eur. J. Org. Chem.* **2012**, *2012*, 3199–3217.
[95] Niu, W. F.; Guo, L.; Li, Y. H.; Shuang, S. M.; Dong, C.; Wong, M. S. Highly selective two-photon fluorescent probe for ratiometric sensing and imaging cysteine in mitochondria. *Anal. Chem.* **2016**, *88*, 1908–1914.
[96] Jiang, L. R.; Hu, Q.; Chen, T. H.; Min, D. Y.; Yuan, H. Q.; Bao, G. M. Highly sensitive and rapid responsive fluorescence probe for determination of formaldehyde in seafood and *in vivo* imaging application. *Spectrochim. Acta Part A* **2020**, *228*, 117789.
[97] Ding, N.; Li, Z.; Hao, Y. T.; Zhang, C. X. Design of a new hydrazine moiety-based near-infrared fluorescence probe for detection and imaging of endogenous formaldehyde *in vivo*. *Anal. Chem.* **2022**, *94*, 12120–12126.
[98] Wang, P. Z.; Cheng, X. H.; Xiong, J. H.; Mao, Z. Q.; Liu, Z. H. Revealing formaldehyde fluxes in Alzheimer's disease brain by an activity-based fluorescence probe. *Chin. J. Chem.* **2022**, *40*, 1457–1463.